

Extra-atomic Relaxation and Core-Level Binding Energy Shifts at Silicon/Silicon Oxide Interfaces: Effects of Cluster Size on Physical Models

K. Z. Zhang and M. M. Banaszak Holl*

Chemistry Department, University of Michigan, Ann Arbor, Michigan 48109-1055

F. R. McFeely

IBM T. J. Watson Research Center, P.O. Box 218, Yorktown Heights, New York 10598

Received: October 7, 1997; In Final Form: December 21, 1997

The Si 2p and O 1s core-level photoemission peaks and the valence band peaks for silicon oxide films grown on crystalline silicon have been observed to shift to higher binding energy as a function of increasing film thickness. The physical basis for this shift has been ascribed to a variety of mechanisms including initial state effects, final state effects, and extrinsic effects. By constructing a structurally homogeneous silicon oxide film consisting of $\text{H}_{10}\text{Si}_{10}\text{O}_{15}$ on silicon, initial state effects have been minimized and the magnitude of final state effects directly measured. Unlike previous studies utilizing the $\text{H}_8\text{Si}_8\text{O}_{12}$ cluster, the cluster precursor utilized in these studies is large enough to allow direct observation of the theoretically predicted asymptotic behavior in the core-level shift as a function of cluster layer thickness prior to the onset of film charging.

I. Introduction

Silicon/silicon oxide interfaces play a central role in modern metal oxide semiconductor (MOS) devices.¹ Physical properties of this interface are of crucial importance in the electrical switching process that allows information to be stored in transistor devices. However, the potentials applied to the thin silicon oxide films that form the gate in MOS devices can lead to chemical reactions occurring in the film and/or in the interface region, ultimately causing electrical breakdown and device failure. These chemical reactions have become increasing problematic as MOS devices have been scaled to ever smaller dimensions. The silicon oxide films currently under investigation for use as gate dielectrics, as thin as 10 Å, are entirely interfacial in nature and no longer have the physical, electrical, or chemical properties of bulk SiO_2 . These developments in device technology and the complex nature of the interfacial oxide have spurred spectroscopic studies designed to investigate the structure and reactivity of the Si/SiO₂ interface region. In this paper, the effects of silicon oxide film thickness upon the observed binding energy (BE) shift of the Si 2p core level will be investigated. In principle, X-ray photoemission spectroscopy (XPS) studies of silicon/silicon oxide interfaces offer an excellent method for characterization of the structure and reactivity of silicon/silicon oxide interfaces.¹ However, in practice, the large change in dielectric constant between Si (12) and SiO₂ (4) complicates BE assignments because of the large change in final-state stabilization energy as a function of the position of a silicon fragment with respect to the interface. Further complicating the issue, the BE shifts observed experimentally as a function of silicon oxide film thickness have variously been ascribed to a wide variety of initial state effects (Si–O ring size, strain, stoichiometry, and crystallinity),² final state effects (various screening mechanisms),³ and extrinsic effects (charging)⁴ that all have the potential to contribute in whole or in part to cause the observed BE shift as the overlayer grows. In fact, all three mechanisms have been invoked over

the past 20 years as sufficient to provide a complete explanation of the distance-dependent shift, and all three explanations continue to be championed in the recent literature. This problem was recently addressed in an experimental modeling study that utilized the hydrospherosiloxane cluster $\text{H}_8\text{Si}_8\text{O}_{12}$ to make structurally homogeneous silicon oxide films.⁵ This study concluded that a significant BE shift of 0.6 eV occurred due to final state stabilization over the silicon oxide thickness regime between 6 and 30 Å (Figure 1, region A). The study was able to rule out charging as an operative BE shift mechanism in this thickness range, although films greater than 30 Å were observed to charge (Figure 1, region B). These conclusions, although firmly grounded by the data acquired using the model $\text{H}_8\text{Si}_8\text{O}_{12}$ -derived films, are at odds with conclusions reached in previous studies.⁶ The importance of understanding the spectroscopic issues relevant to silicon/silicon oxide interfaces have prompted us to vary the model system by increasing the cluster size. The electron-transport and classical electrostatic theories used to explain the behavior of the $\text{H}_8\text{Si}_8\text{O}_{12}$ -derived films predict that charging should occur at roughly the same number of cluster layers but that the overall BE shift should be greater per layer because the larger cluster moves the average HSiO_3 fragment farther from the bulk silicon. The use of a larger cluster allows an additional test of the BE shift mechanisms ascribed to regions A and B in Figure 1. To test these hypotheses, $\text{H}_{10}\text{Si}_{10}\text{O}_{15}$ (Figure 2), the next largest spherosiloxane cluster, was physisorbed onto a chemisorbed layer of $\text{H}_{10}\text{Si}_{10}\text{O}_{15}$ on Si(100). Spherosiloxane clusters make close to ideal test systems because the physisorbed films can be varied in thickness while maintaining exactly the same bonding environment about all of the silicon atoms.⁷ Thus, the initial state and final state effects upon the BE shift in the cluster-derived thin oxide films is decoupled, unlike the case in amorphous silicon oxide films on silicon where the structure of the silicon oxide is uncertain, and initial and final state effects are convoluted in an undetermined fashion. On the basis of a comparison to the closely related hydrosils-

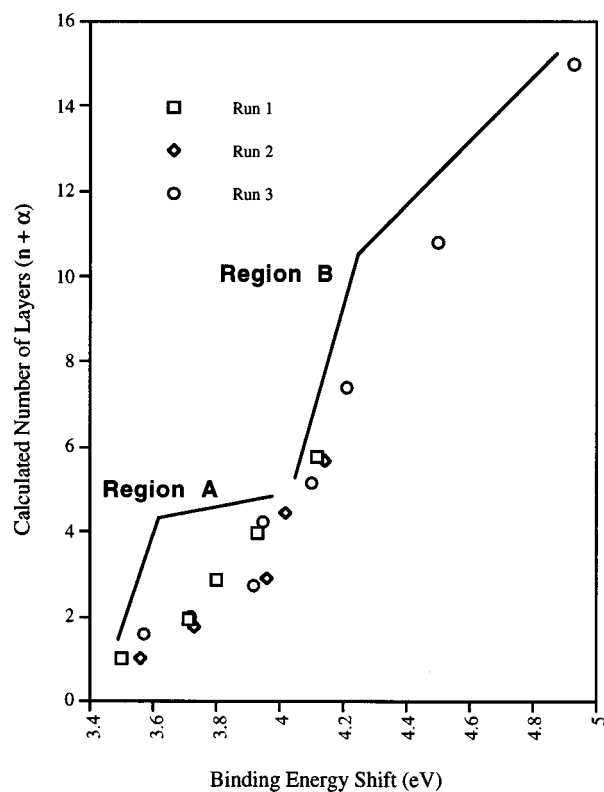


Figure 1. Binding Energy (BE) shift vs number of cluster layers ($n+\alpha$) for three silicon oxide films derived from the physisorption of $\text{H}_8\text{Si}_8\text{O}_{12}$ on $\text{Si}(100)$. In region A, final state effects in the form of extra-atomic relaxation cause the BE shift. In region B, charging of the film is occurring.

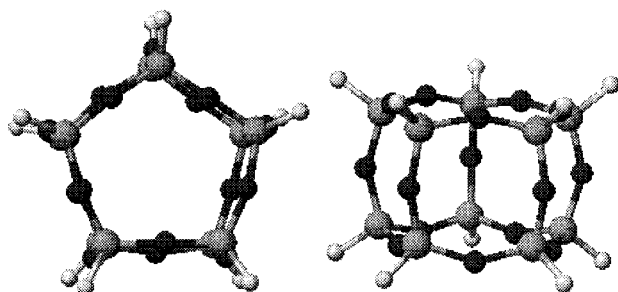


Figure 2. Two views of the $\text{H}_{10}\text{Si}_{10}\text{O}_{15}$ spherosiloxane cluster.

esquioxane polymers, these films should have a dielectric constant between 3 and 4,⁸ similar to SiO_2 . It should also be pointed out that the use of molecular-based films, as opposed to thermal or deposited silicon oxide films, is irrelevant with respect to the image charge ideas used to explain the final state stabilization effects. The image charge stabilization calculations include only the dielectric constant of the material and do not require or take into account any detailed aspects of film structure.

The results obtained provided experimental support for the following conclusions: (1) extra-atomic final state effects have been observed to play the dominant role in causing thickness-dependent BE shifts at silicon/silicon oxide interfaces for films ranging from 0 to ~ 30 – 40 Å; (2) the magnitude of this effect is measured by this experiment to be at least 0.4 eV, and we estimate the maximum possible effect in the Si/SiO_2 system to be about 1 eV; (3) charging occurs in both the $\text{H}_8\text{Si}_8\text{O}_{12}$ - and $\text{H}_{10}\text{Si}_{10}\text{O}_{15}$ -derived model interfaces when the number of cluster layers exceeds ~ 5 layers or about 30 and 40 Å, respectively; (4) initial state effects play a negligible role in the observed thickness-dependent BE shifts for both the model interfaces and

for the SiO_4 fragments assigned to the peak at ~ 3.6 – 4.0 eV in Si/SiO_2 interfaces. In addition, the results show the trends expected for a larger cluster based on classical electrostatics and expected electron-transport behavior.

II. Experimental Section

The hydridospherosiloxane cluster $\text{H}_{10}\text{Si}_{10}\text{O}_{15}$ was synthesized via the method of Agaskar and sublimed.⁹ Single-layer coverage of the clusters on $\text{Si}(100)-2 \times 1$ was achieved by dosing a clean $\text{Si}(100)-2 \times 1$ crystal with the vapor of $\text{H}_{10}\text{Si}_{10}\text{O}_{15}$ in ultrahigh vacuum (UHV) as previously described.¹⁰ Multilayer films of condensed $\text{H}_{10}\text{Si}_{10}\text{O}_{15}$ clusters were prepared by cooling the substrates to approximately -165 °C and exposing to the vapor of $\text{H}_{10}\text{Si}_{10}\text{O}_{15}$ ($\sim 2 \times 10^{-7}$ Torr). A manipulator capable of being cooled to -165 °C using liquid N_2 was fitted to a chamber pumped with a turbomolecular pump (base pressure 1×10^{-10} Torr), separated from the spectrometer chamber by a gate valve. The silicon sample was fixed to the copper manipulator over a sapphire plate (for electrical insulation) using Ta foil. In all cases, sample cleanliness was verified by checking the Si 2p and C 1s core levels and the valence band region. Of particular concern was the possibility of trace water derived from the UHV chamber coadsorbing on the substrate over the time period of the experiment. However, monitoring the valence band region indicated no change in the relative intensity of the O 2p “lone-pair” feature at ~ -8 eV versus the cluster-derived H–Si and Si–O features in the -9 to -18 eV region, ruling out water condensation as a significant problem. Soft X-ray photoemission spectra were obtained at the National Synchrotron Light Source at Brookhaven National Laboratory as previously described.^{10b} The photoemission spectra were obtained at 170, 300, and 400 eV incident photon energy. These energies were selected to maximize surface selectivity and vary the electron escape depths while at the same time allowing direct integration of the observed core-level peaks. Core-level Si 2p spectra were treated as previously described by Himpsel et al.¹¹ A spin–orbit coupling ratio of 0.5 and an energy separation of 0.6 eV were employed to remove the Si $2p_{1/2}$ component for the spectra presented.

III. Results

The initial layer of $\text{H}_{10}\text{Si}_{10}\text{O}_{15}$ clusters on $\text{Si}(100)-2 \times 1$ was formed via chemisorption.^{10c} Monolayer oxide films of this type do not charge as has been discussed in detail previously.⁵ Silicon oxide films of varying thickness were formed by physisorbing $\text{H}_{10}\text{Si}_{10}\text{O}_{15}$ clusters at -165 °C onto a surface already containing a chemisorbed layer. A series of spectra at 170, 300, and 400 eV incident photon energy were collected as a function of cluster dose (Figure 3 and Table 1). Note the shift of peak III by approximately 0.5 eV as a function of cluster dose and average layer thickness.¹² Calculation of average layer thickness requires quantitative measurement of the attenuation factor for the emitted photoelectrons which can be related to electron escape depth and film thickness. The monolayer attenuation factor is obtained for each photon energy by measuring the area of the Si 2p core-level peaks for a clean $\text{Si}(100)-2 \times 1$ sample (the “bulk” and all surface states) and dividing this by the area of the Si 2p core-level peaks derived from the substrate (features labeled “bulk” and I in Figure 3) after one layer of clusters has been chemisorbed. The monolayer attenuation factors were calculated to be 0.51 (1), 0.64 (2), and 0.78 (8) for 170, 300, and 400 eV, respectively.¹³ The experimentally measured ratio of the areas for the bulk silicon derived peaks ($I_{n+\alpha}^s$) divided by the cluster derived peak areas

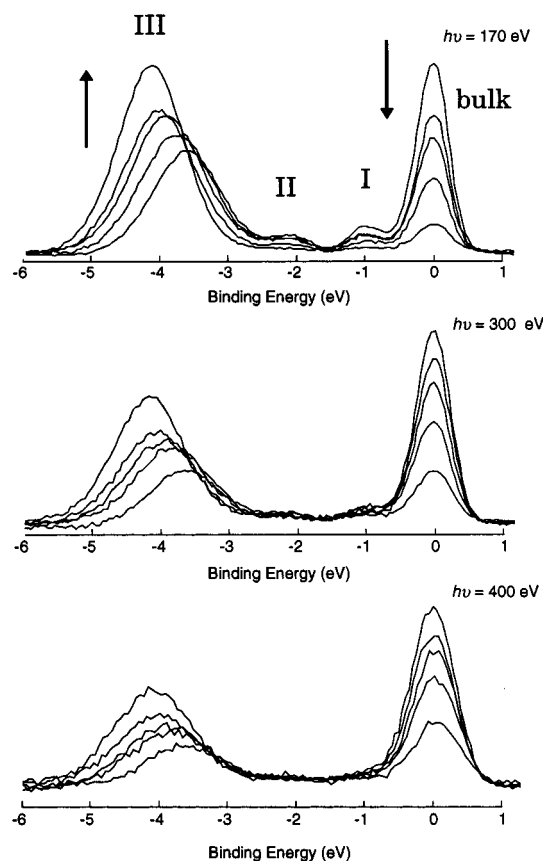


Figure 3. Soft X-ray Si $2p_{3/2}$ core-level photoemission spectra of varying thickness $H_{10}Si_{10}O_{15}$ films on a Si(100) substrate. Panel (a): 170 eV. Panel (b): 300 eV. Panel (c): 400 eV.

TABLE 1: Data for Multiphoton Energy Experiment of Physisorption of $H_{10}Si_{10}O_{15}$ on Chemisorbed Layer Corresponding to Figure 5

dose (Torr s)	photon energy	ratio (I_s/I_c)	no. of layers ($n + \alpha$) (average) ^a	shift of $HSiO_8$ feature (eV)
9.4×10^{-6}	170	0.92	1	3.6
	300	1.67		3.6
	400	2.17		3.6
1.6×10^{-5}	170	0.52	1.6(1)	3.8
	300	1.02		3.9
	400	1.44		3.8
2.8×10^{-5}	170	0.40	1.8(1)	3.9
	300	0.79		4.0
	400	1.15		4.0
1.3×10^{-4}	170	0.26	2.3(1)	4.0
	300	0.59		4.0
	400	0.87		4.0
	170	0.072	3.9(3)	4.1
	300	0.24		4.2
	400	0.39		4.1

^a The number of layers is the average of the values derived from the intensity ratios observed in the 170, 300, and 400 eV spectra.

($I_{n+\alpha}^c$) can be related to the number of cluster layers ($n + \alpha$) by eq 1.¹⁴

$$R(n+\alpha) = \frac{I_{n+\alpha}^s}{I_{n+\alpha}^c} = \left[\frac{(1-\alpha)e^{-\xi n} + \alpha e^{-\xi(n+1)}}{(1-\alpha) \sum_{i=0}^{n-1} e^{-\xi i} + \alpha \sum_{i=0}^n e^{-\xi i}} \right] \frac{I_{(0)}^s}{I_{(1)}^c} \quad (1)$$

The thickness of each layer can be estimated by examining the interlayer distances in crystalline $H_{10}Si_{10}O_{15}$.¹⁵ Intermolecular

TABLE 2: Data for Physisorption of $H_{10}Si_{10}O_{15}$ on Chemisorbed Layer (170 eV corresponding to Figure 7)

spectrum	dose (Torr s)	ratio ($I_{n+\alpha}^s/I_{n+\alpha}^c$)	no. of layers ($n + \alpha$)	shift of $HSiO_3$ feature (± 0.1 eV)	fwhm $HSiO_3$ feature (± 0.1 eV)
1		0.97	1.0	3.58	1.14
2	1.4×10^{-5}	0.59	1.5	3.70	1.15
3	2.8×10^{-5}	0.54	1.6	3.78	1.18
4	5.0×10^{-5}	0.28	2.3	3.81	1.16
5	6.5×10^{-5}	0.20	2.7	3.91	1.18
6	8.1×10^{-5}	0.13	3.2	3.93	1.16
7	9.9×10^{-5}	0.087	3.7	3.94	1.15
8	1.2×10^{-4}	0.068	4.0	3.98	1.12
9	1.5×10^{-4}	0.039	4.9	4.01	1.13
10	1.9×10^{-4}		6.0 ^a	4.24	1.18
11	2.7×10^{-4}		7.9 ^a	4.47	1.28
12	3.8×10^{-4}		10.7 ^a	4.75	1.41

^a These values are based on a linear extrapolation of data because the intensity of the substrate peak was too small to measure.

contact distances vary somewhat so an average distance of ~ 8 Å was used for purposes of estimating film thickness from a calculated number of cluster layers. The physisorbed films for the spectra in Figure 3 are estimated to be between 8 and ~ 30 Å thick.

The BE shift as a function of film layer thickness was studied over a greater thickness range using a 170 eV incident photon energy. This photon energy gives high signal-to-noise data in which all the Si 2p core-level peaks have essentially identical cross-section values. In addition, high-quality valence band spectra can be obtained at this photon energy. The data for this experiment are shown in Figure 4 and summarized in Table 2. The peaks labeled bulk, I, and II in panel (b) decrease in intensity as the substrate and initial chemisorbed layer derived peaks are attenuated by an increasingly thick physisorbed film. However, peak III, derived from the $HSiO_3$ fragments of the initial chemisorbed layer and the intact $H_{10}Si_{10}O_{15}$ clusters of the physisorbed layers, increases in area and shifts to higher binding energy until the dose reaches 1.5×10^{-4} Torr, equivalent to ~ 5 layers or a thickness of ~ 40 Å. After this point, although the peak continues to shift to higher binding energy and peak area continues to increase in a linear fashion with cluster dose (Figure 5), peak height begins to decrease as the full width at half-maximum (fwhm) begins to dramatically increase. The valence band spectra shown in panel (a) shows the same shift as a function of film thickness and the features also begin to show a greater fwhm at the same thickness as the Si 2p core-level spectra. Broadening of peaks in this fashion is generally associated with sample charging. The peaks become broader because of the inhomogeneous distribution of charge in the oxide film.¹⁶ Note that the Si 2p core-level for the bulk silicon does not show an increase in fwhm or shift, indicating that just the oxide film is charging, not the whole sample. Additional evidence that the behavior of peak III is caused by charging comes from the time dependence of the BE shift. Peak III in physisorbed films such as spectra 11 and 12 in Figure 4 slowly broadens and shifts over a period of about 40 min (Figure 6). However, for the thinner films shown in region (a) of Figure 4, no such time dependence is observed for the BE shift or fwhm.⁵

A plot of BE shift versus number of layers is shown in Figure 7 for two separate physisorption experiments. Two distinct regions can be observed in this plot. Region A corresponding to the spectra in which the BE shifts but the fwhm does not change (spectra 1–8), and region B corresponding to the spectra for which the BE shifts and the fwhm increases (spectra 9–12).

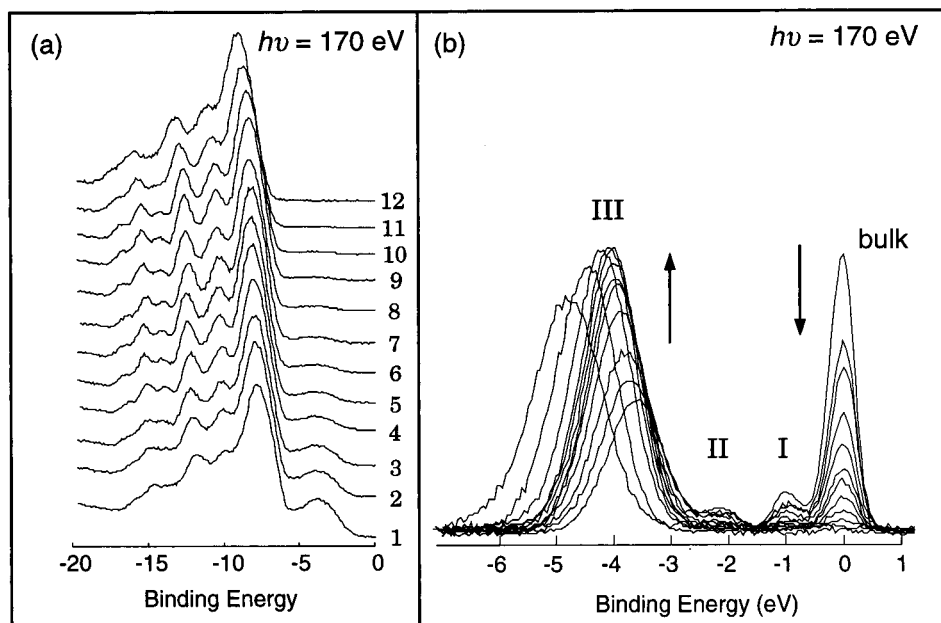


Figure 4. Soft X-ray photoemission spectra of $\text{H}_{10}\text{Si}_{10}\text{O}_{15}$ derived films varying in thickness from 8 to 90 Å. Panel (a): valence band spectra numbered corresponding to Table I. Panel (b): Si $2p_{3/2}$ core-level spectra.

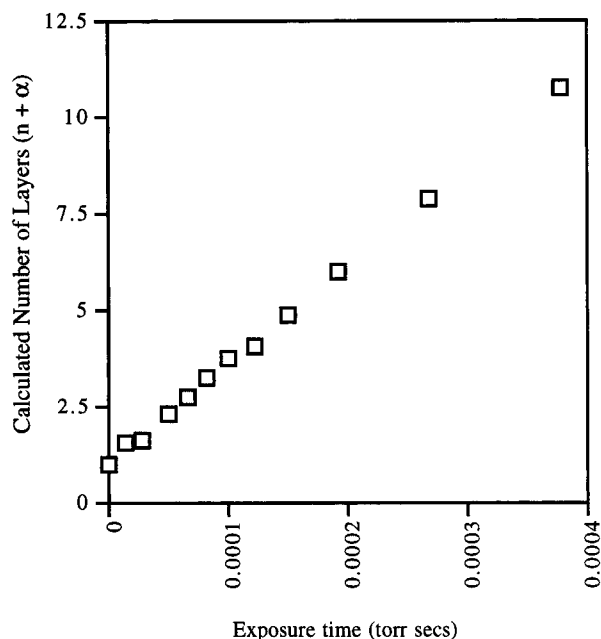


Figure 5. Exposure time vs number of cluster layers ($n + \alpha$) corresponding to the data presented in Figure 4 and Table II.

For a given layer thickness, a standard deviation of ~ 0.1 eV is observed. These values give a good indication of the reproducibility of the experiment and the errors associated with data collection and analysis.

IV. Discussion

In a previous study examining physisorbed films of $\text{H}_8\text{Si}_8\text{O}_{12}$ on Si(100), a detailed discussion relating this type of experiment to issues of charging and BE shifts for Si/SiO₂ interfaces was provided.⁵ These arguments will not be repeated here, except to note that the experiments reported in this paper using physisorbed films of $\text{H}_{10}\text{Si}_{10}\text{O}_{15}$ clusters are in agreement with and support the previous conclusions. Instead, the discussion will focus on the observed differences between $\text{H}_8\text{Si}_8\text{O}_{12}$ - and $\text{H}_{10}\text{Si}_{10}\text{O}_{15}$ -derived films and how these differences relate to theoretical ideas regarding final state stabilization mechanisms.

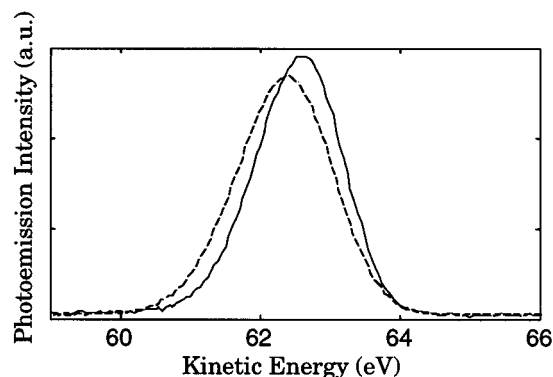


Figure 6. BE as a function of soft X-ray exposure time for a thick physisorbed film ~ 80 Å thick. Dashed line spectrum taken after 40 minutes additional X-ray exposure. Solid line FWHM = 1.46 eV. Dashed line FWHM = 1.61 eV. BE shift is 0.27 eV.

Extra-atomic final state stabilization, resulting in a reduction of the measured BE, decreases as a function of the distance of the emitting silicon fragment from the bulk silicon. Classical electrostatic theory predicts that this decrease should be in the form of an exponential curve. Both Browning et al. and Pasquarello et al. have previously discussed this issue in detail, giving the appropriate equation and plots for various thicknesses.^{17,18} Unfortunately, it was not clear from the data obtained for the $\text{H}_8\text{Si}_8\text{O}_{12}$ -derived films if the expected exponential behavior was being observed.⁵ The rate of change of BE as a function of number of cluster layers did not reach an asymptotic limit prior to the onset of charging. Charge dissipation in an insulating film constructed of discrete clusters is expected to depend strongly on the number of layers and only weakly on the absolute thickness for clusters of similar size. This is because charge transport within a cluster should be fast as compared to charge hopping between clusters. Thus, when using a spherosiloxane cluster larger than $\text{H}_8\text{Si}_8\text{O}_{12}$, the average observed BE shift should be larger per layer, but the sample should still charge at roughly the same number of layers. The phenomenon should make possible observation of the exponential behavior of BE as a function of distance from the bulk silicon if the chosen cluster is large enough. The expected

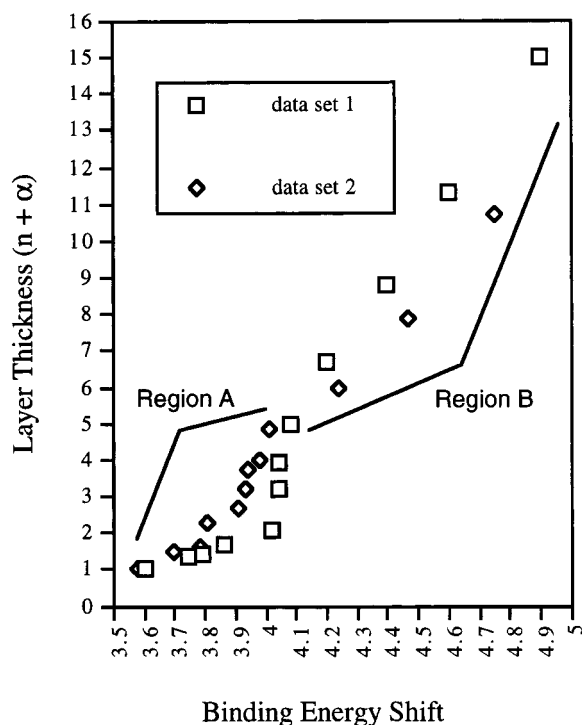


Figure 7. BE shift vs number of cluster layers ($n \times \alpha$) for two runs. Data set 2 corresponds to Table II.

approach to a limit in the amount of BE stabilization as a function layer thickness is clearly observed in Figure 7. The observed binding energy shift caused by final state stabilization for this system is 0.4 eV over approximately 30 Å. This is smaller than the 0.6 eV shift observed for the system based on $\text{H}_8\text{Si}_8\text{O}_{12}$ films,⁵ as expected since the initial physisorbed layer for the $\text{H}_{10}\text{Si}_{10}\text{O}_{15}$ films begins ~8 Å from the bulk Si as opposed to ~6 Å for the $\text{H}_8\text{Si}_8\text{O}_{12}$ films.

As indicated by the fwhm of both the valence band and Si 2p core-level spectra, the onset of charging for the $\text{H}_{10}\text{Si}_{10}\text{O}_{15}$ -derived films is at ~5 layers or approximately 40 Å thickness. By way of comparison, the onset of charging for the $\text{H}_8\text{Si}_8\text{O}_{12}$ -derived films also began at ~5 layers or approximately 30 Å thickness,⁵ consistent with the expectation that the rate-limiting step should be intercluster charge transfer. Thus, as expected, charging appears more sensitive to the number of cluster layers than the actual film thickness. Of course, the amorphous SiO_2 (*a*- SiO_2) films used in device Si/ SiO_2 interfaces are not composed of clusters and so will not have the same type of intercluster hopping mechanism limiting the charge-transport rate. Based on the trend in the cluster data and the lower dielectric constant for the clusters as compared to *a*- SiO_2 ,⁵ the expectation would be for the rate of charge transport to be greater in *a*- SiO_2 films than in the cluster-derived films. If these assumptions hold, the cluster data imply that *a*- SiO_2 films should not charge until at least 30–40 Å thick when studied under X-ray fluxes similar to those used in this experiment.

V. Conclusions

Physisorption of spherosiloxane clusters onto Si(100) substrates provides a useful method of making structurally homogeneous silicon oxide films of varying thickness. Photoemission studies of these films indicate two separate thickness ranges over which different physical mechanisms cause the observed thickness-dependent BE shift. Over the range 0 to ~5 layers (30–40 Å), the BE shift is caused by extra-atomic final state

stabilization of the core level by the polarizable silicon substrate. Once the thickness exceeds ~5 cluster layers, charging of the silicon oxide film occurs, resulting in an accompanying increase in fwhm. After the onset of charging, the relative magnitudes of the extra-atomic relaxation and charging effects upon the observed shift can no longer be experimentally deconvoluted. The observed shape of the curve for the final state stabilized region is consistent with expectations based upon classical electrostatic theory.^{17,18} The model films presented in this study and the analogous study performed previously⁵ clearly demonstrate the importance of explicitly accounting for extra-atomic relaxation effects when assigning the BE shift of a Si 2p core level to a structural moiety. The consequences of ignoring the important role of extra-atomic relaxation include the erroneous assignment of the BE shift to a variety of structurally based mechanisms such as Si–O ring size, film stoichiometry, and film strain.⁶ In a general sense, explicit consideration of extra-atomic relaxation is clearly crucial whenever photoemission is used to study solid/solid interfaces of two solids with greatly differing dielectric constants. In the area of microelectronic device materials characterization, these considerations are of increasing importance as device length scales continue to decrease, and the device materials become dominated by interfacial properties.

Acknowledgment. This work was supported by grants from the National Science Foundation (DMR-9727166) and IBM (to M.M.B.H.). Portions of this work were carried out at the National Synchrotron Light Source, Brookhaven National Laboratory, which is supported by the Department of Energy (Division of Materials Science and Division of Chemical Sciences).

References and Notes

- (1) For lead references see: (a) *The Physics and Chemistry of SiO_2 and the Si– SiO_2 Interface 2*; Massoud, H. Z.; Poindexter, E. H.; Helms, C. R., Eds.; Electrochemical Society: Pennington, NJ, 1996. (b) *The Physics and Chemistry of SiO_2 and the Si– SiO_2 Interface 2*; Helms, C. R.; Deal, B. E. Eds.; Plenum: New York, 1993. (c) *The Physics and Technology of Amorphous SiO_2* ; Devine, R. A. B. Eds.; Plenum: New York, 1988. (d) *SiO_2 and Its Interfaces*; Pantelides, S. T.; Lucovsky, G. G., Eds.; Mater. Res. Soc. Symp. Proc., 1990. (e) *The Physics and Technology of Amorphous Silicon Dioxide*; Helms, C. R.; Deal, B. E., Eds.; Plenum: New York, 1989.
- (2) Initial state effects refer to structural and compositional features of the material that influence the energy level of the core state prior to interaction with the exciting photon. In general, any change that effects the valence electron distribution will also cause the energy of the core electrons to vary.
- (3) Final state effects refer to mechanisms that serve to stabilize (or destabilize) the positively charged core–hole state that is formed upon ejection of the photoelectron from the emitting atom.
- (4) Extrinsic effects are defined as those not related to the specific geometric or electronic structure of the material to be studied but instead related to details of the experimental conditions. For example, charging occurs when insulating samples are exposed to an X-ray source.
- (5) Zhang, K. Z.; Greeley, J. N.; Banaszak Holl, M. M.; McFeely, F. R. *J. Appl. Phys.* **1997**, *82*, 2298.
- (6) For detailed discussions of alternative interpretations and lead references see: (a) Iwata, S.; Ishizaka, A. *J. Appl. Phys.* **1996**, *79*, 6653. (b) Hattori, T. *Crit. Rev. Sol. State Mater. Sci.* **1995**, *20*, 339. (c) Grunthaner, F. J.; Grunthaner, P. J. *Mater. Sci. Rep.* **1986**, *1*, 65.
- (7) For a detailed discussion of this issue see the experimental design section in ref 5.
- (8) Hacker, N. P. *MRS Bull.* **1997**, *22*, 33.
- (9) (a) Agaskar, P. A. *Inorg. Chem.* **1991**, *30*, 2707. (b) Agaskar, P. A.; Klemperer, W. G. *Inorg. Chim. Acta* **1995**, *229*, 355. (c) Frye, C. L.; Collins, W. T. *J. Am. Chem. Soc.* **1970**, *92*, 5586.
- (10) (a) Banaszak Holl, M. M.; McFeely, F. R. *Phys. Rev. Lett.* **1993**, *72*, 2441. (b) Lee, S.; Maken, S.; Banaszak Holl, M. M.; McFeely, F. R. *J. Am. Chem. Soc.* **1994**, *116*, 11819. (c) Zang, K. Z.; Meeuwenberg, L. M.; Banaszak Holl, M. M.; McFeely, F. R. *Jpn. J. Appl. Phys.* **1997**, *36*, 1622.

(11) (a) Himpsel, F. J.; McFeely, F. R.; Taleb-Ibrahimi, A.; Yarmoff, J. A.; Hollinger, G. *Phys. Rev. B* **1988**, 38, 6084.

(12) The following discussion briefly explains the methods and numerical values used in this paper. For a detailed discussion of the approach taken, the assumptions made, and derivation of equations see ref 5.

(13) The reported value is the average of three runs. The standard deviation is given in parentheses.

(14) n = the number of completed layers and α = the fractional completion of a layer.

(15) Bürgi, H.-B.; Törnroos, K. W.; Calzaferri, G.; Bürgy, H. *Inorg. Chem.* **1993**, 32, 4914.

(16) *Practical Surface Analysis*, 2nd ed.; Briggs, D., Seah, M. P., Eds.; Wiley: New York, 1990.

(17) Browning, R. Sobolewski, M. A.; Helms, C. R. *Phys. Rev. B* **1988**, 38, 13407.

(18) Pasquarello, A.; Hybertson, M. S.; Car, R. *Phys. Rev. B* **1996**, 53, 10942.